C. R. Mecanique 344 (2016) 642–648

Contents lists available at ScienceDirect

Comptes Rendus Mecanique

www.sciencedirect.com

Divergence-free condition in transport simulation

Adrien Berchet, Anthony Beaudoin *, Serge Huberson

Institute of Pprime, SP2MI-Téléport 2, boulevard Marie-et-Pierre-Curie, BP 30179, 86962 Futuroscope Chasseneuil-du-Poitou cedex, France

ARTICLE INFO

Article history:
Received 25 July 2015
Accepted 5 February 2016
Available online 4 July 2016

Keywords:
Divergence-free condition
Particle method
Renormalization method
Relaxation method

ABSTRACT

In this work, two adaptations of the particle method allowing one to reduce the numerical errors induced by the non-zero divergence of flow fields in the numerical simulations of particle transport are presented. The first adaptation is based on the renormalization method allowing one to use an irregular distribution of particles induced by the non-zero divergence of flow fields. The second adaptation consists in applying a correction on the weight of the particles by using the relation between the divergence of flow fields and the particles' volume evolution. This adaptation may be considered as a relaxation method. The accuracy of both methods is evaluated by simulating the transport of an inert tracer by the flow of a jet in crossflow whose concentration fields were measured experimentally. The comparison between the numerical and experimental results shows clearly that the two adaptations of the particle method correct efficiently the effect of a non-zero divergence velocity field on the computed concentration.

1. Introduction

The numerical simulations of particle transport involves several difficulties, which have been widely addressed, particularly that of the numerical stability. Among the numerous discretization methods proposed to solve this problem, those using Lagrangian coordinates have a particular place since they usually yield new difficulties while naturally solving the stability issue. Using particles requires the computation of their trajectories, which can be readily achieved with a Runge–Kutta high-order scheme. However, the results have been found to be very sensitive to the quality of the velocity field approximation, particularly regarding the satisfaction of the divergence-free condition. Such errors result in the existence within the flow field of sources and sinks which in some cases yield non-physical crossing trajectories [1,2]. Another consequence is the non-uniformity of the particle distribution, which implicitly yields particles with non-constant volume or surface [3,4]. The solution to these problems requires the design of specific solutions, particularly when the Lagrangian coordinates are used to solve the flow equations. There are basically two families of particle methods used for the flow simulation: the SPH method [5,6], and the vortex method [7,8]. In both cases, some methods have been proposed to overcome the non-divergence-free problem. In the last case, the difficulty is even greater for three-dimensional flows because not only the velocity field, but also the vorticity field as well, must be divergence free. In this paper, we consider the rather different and somewhat simpler problem of the transport of inert tracer particles by a given flow field. This flow can result either from a numerical CFD calculation or of an experimental PIV velocity field. In both cases, the divergence is only approximately zero and techniques derived from the previously mentioned works can be applied. These two different ways to solve this problem are described hereafter and tested on a measured 3D velocity field [9,10].

* Corresponding author.
E-mail address: anthony.beaudoin@univ-poitiers.fr (A. Beaudoin).

http://dx.doi.org/10.1016/j.crme.2016.02.007

2. Particle method

2.1. Approximated concentration field

As usual in the particle method, the concentration field $c(\mathbf{x},t)$ is discretized in a set of numerical particles. Each particle $\mathcal{P}_i$ is defined by its location $\mathbf{X}_i(t)$ and its weight $C_i(t)$:

$$\mathbf{X_i}(t) = \int_{\sigma_i} \mathbf{x}(t)\,\mathrm{d}v \Big/ \int_{\sigma_i} \mathrm{d}v \quad \text{and} \quad C_i(t) = \int_{\sigma_i} c(\mathbf{x},\mathbf{t})\,\mathrm{d}v \tag{1}$$

where σ_i denotes the support surface or volume of the particle $\mathcal{P}_i$. σ_i is usually constant for an incompressible flow. Thanks to the particle discretization, the concentration field $c(\mathbf{x},t)$ can be estimated by means of a sum of products of weight $C_i(t)$ and Dirac measure $\delta(\mathbf{x})$:

$$c(\mathbf{x},t) = \int_{R^d} c(\mathbf{x}',t)\,\delta(\mathbf{x}'-\mathbf{x}) = \sum_i C_i(t)\,\delta(\mathbf{X}_i(t)-\mathbf{x}) \tag{2}$$

where d is the space dimension. In order to obtain a continuous approximation of the concentration field $c_h(\mathbf{x},t)$, the Dirac measure $\delta(\mathbf{x})$ is approximated by a smooth function $\zeta_\epsilon(\mathbf{x})$ in the previous equation:

$$c_h(\mathbf{x},t) = \sum_i C_i(t)\,\zeta_\epsilon(\mathbf{X}_i(t)-\mathbf{x}) \quad \text{with} \quad \zeta_\epsilon(\mathbf{x}) = (1/\epsilon^d)\zeta(\mathbf{x}/\epsilon) \tag{3}$$

where ϵ is the smoothing parameter proportional to the diameter of the numerical particles. In order to check the consistency of Eq. (3), the smoothing function $\zeta_\epsilon(\mathbf{x})$ has to satisfy momentum conditions:

$$\int_{\mathcal{R}^d} \zeta_\epsilon(\mathbf{x})\,\mathrm{d}\mathbf{x} = 1 \quad \text{and} \quad \int_{\mathcal{R}^d} \mathbf{x}\zeta_\epsilon(\mathbf{x})\,\mathrm{d}\mathbf{x} = 1 \tag{4}$$

As the approximated concentration field $c_h(\mathbf{x},t)$ is a sum of products of $C_i(t)$ and $\zeta_\epsilon(\mathbf{X}_i(t)-\mathbf{x})$, an irregular particle distribution will lead to a shaky approximation of the concentration field $c_h(\mathbf{x},t)$.

2.2. Lagrangian transport equations

In the case of pure advection, the transport equation of an inert tracer can be written as follows:

$$\frac{\partial c(\mathbf{x},t)}{\partial t} + \nabla(\mathbf{u}(\mathbf{x},t)c(\mathbf{x},\mathbf{t})) = 0 \tag{5}$$

where $\mathbf{u}(\mathbf{x},t)$ is the velocity field. In the particle method, this transport equation is written in a Lagrangian framework yielding the discrete approximation:

$$\frac{\mathrm{d}\mathbf{X}_i(t)}{\mathrm{d}t} = \mathbf{u}(\mathbf{X}_i,t) \quad \text{and} \quad \frac{\mathrm{d}C_i(t)}{\mathrm{d}t} = 0 \tag{6}$$

The first equation can be numerically solved by using a 4th-order accurate Runge–Kutta scheme. As the transport equation is an advection equation (Eq. (5)), the weight $C_i(t)$ of a numerical particle $\mathcal{P}_i$ is constant (Eq. (6), right). Thus the particle method is a conservative method in this case.

2.3. Renormalized smoothing function

The discrete form of the first moment condition (Eq. (4), left) reads:

$$\mathbf{1}(\mathbf{x},t) = \sum_i \zeta_\epsilon(\mathbf{X}_i(t)-\mathbf{x}) \tag{7}$$

The previous equation is equal to 1 as long as the particle volumes remain constant. This is not the case of flow fields with a non-zero divergence where an irregular particle distribution can appear. This problem has been addressed by Gingold and Monaghan [5,6], who proposed the renormalization method. This method consists in dividing Eq. (3) (left) by the renormalization coefficient $\mathbf{1}(\mathbf{x},t)$ defined by Eq. (7). As a result, the approximated concentration field $c_h(x,t)$ reads:

$$\frac{c_h(\mathbf{x},t)}{\mathbf{1}(\mathbf{x},t)} = \frac{\sum_i C_i(t)\zeta_\epsilon(\mathbf{X}_i(t)-\mathbf{x})}{\sum_i \zeta_\epsilon(\mathbf{X}_i(t)-\mathbf{x})} \tag{8}$$

The renormalization coefficient $\mathbf{1}(\mathbf{x},t)$ accounts for the actual volume variations of numerical particles. In the paper, the renormalization method will be denoted RSF (Renormalized Smoothing Function).

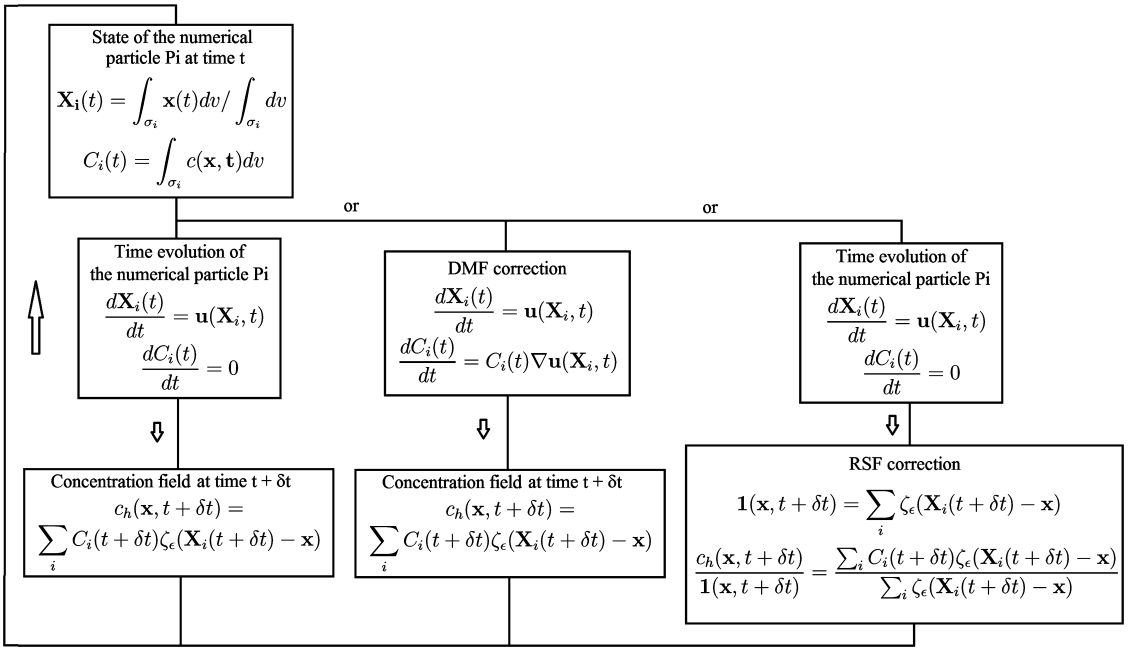

Fig. 1. Numerical algorithm of the particle method with or without the two corrections, DMF (Divergence Mass Flux) and RSF (Renormalization Smoothing Function), used to perform the numerical simulations.

2.4. Divergence mass flux

In the case of flow fields with a non-zero divergence, the transport equation of an inert tracer is no longer equivalent to the advection equation (Eq. (5)), and an additional source term has to be taken into account:

$$\frac{\partial c(\mathbf{x}, t)}{\partial t} + \nabla(\mathbf{u}(\mathbf{x}, t)c(\mathbf{x}, \mathbf{t})) = c(\mathbf{x}, t)\nabla\mathbf{u}(\mathbf{x}, t) \tag{9}$$

Thus the previous set of differential equations (Eq. (6)) becomes:

$$\frac{\mathrm{d}\mathbf{X}_i(t)}{\mathrm{d}t} = \mathbf{u}(\mathbf{X}_i, t) \quad \text{and} \quad \frac{\mathrm{d}C_i(t)}{\mathrm{d}t} = C_i(t)\nabla\mathbf{u}(\mathbf{X}_i, t) \tag{10}$$

The source term of the transport equation (9) can be interpreted as an anti-diffusion one, which corrects the weight $C_i(t)$ of the numerical particle $\mathcal{P}_i$. The simplest scheme for solving Eq. (10) (right) is the first-order Euler scheme:

$$C_i(t+\delta t) = C_i(t) + \delta t C_i(t)\nabla\mathbf{u}(\mathbf{X}_i, t) \tag{11}$$

where δt is the time step. This method is somewhat similar to the relaxation method initially proposed by Beale for the vortex methods [7,8]. In this paper, the relaxation method will be denoted DMF (Divergence Mass Flux).

2.5. Correction methods implementation

The numerical algorithm used to perform the numerical simulations is given in Fig. 1. The main loop consists of the two steps of the particle method without any correction. The first step is the time evolution of the numerical particle $\mathcal{P}_i$ defined by its location $\mathbf{X}_i(t)$ and its weight $C_i(t)$ at time t. This step is performed by solving the set of differential equations (6). At the end of this step, only the location $\mathbf{X}_i(t) \neq \mathbf{X}_i(t+\delta t)$ has changed. The weight $C_i(t) = C_i(t+\delta t)$ is kept constant so far. The second step is the approximation of the concentration field $c_h(\mathbf{x}, t+\delta t)$, which is performed by using Eq. (3) (left).

The RSF correction is then implemented in the numerical algorithm by substituting Eq. (8) for Eq. (3) (left). The RSF correction corrects the effect of the non-zero divergence without modifying the location $\mathbf{X}_i(t+\delta t)$ and the weight $C_i(t+\delta t)$ of the numerical particle $\mathcal{P}_i$. The RSF correction is based on the first-moment condition (Eq. (4), left) that the smoothing function $\zeta_\epsilon(\mathbf{x})$, used in Eq. (3) for the estimation of the concentration field $c_h(\mathbf{x}, t+\delta t)$, has to satisfy. In Eq. (8), the renormalization coefficient $\mathbf{1}(\mathbf{x}, t+\delta t)$, defined in Eq. (7) from the first moment condition (Eq. (4), left), corrects the impact of the distortion induced by the non-zero divergence of flow fields on the set of numerical particles, thus on the approximated concentration.

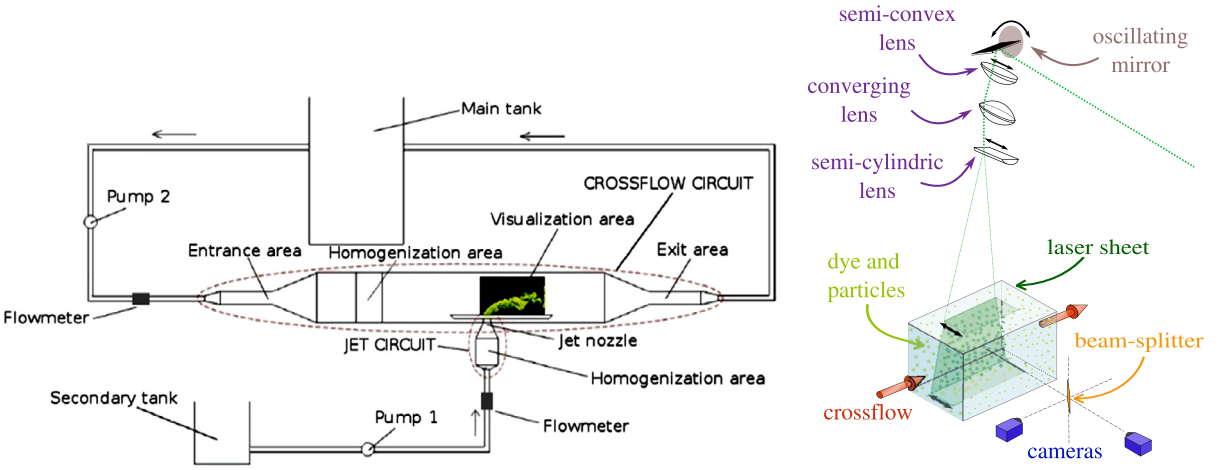

Fig. 2. Experimental setup (left) and measurement techniques (right).

The DMF correction is then implemented to the numerical algorithm by substituting Eqs. (10) by Eqs. (6). In the DMF correction, the weight of the numerical particle $\mathcal{P}_i$ is not constant, $C_i(t) \neq C_i(t+\delta t)$. The numerical solution to the differential equation (10) (right) is obtained by means of a first-order Euler scheme. Eq. (10) (right) discretization yields Eq. (11). Therefore, the accuracy of the DMF correction is sensitive to the time step chosen, δt. There is no cumulative error effect for the RSF method, although it can be expected that the performance of the method can be severely altered for long-time calculations if the particle distribution's regularity is badly deteriorated.

3. Measured velocity field

The transport of inert tracer particles through a jet in crossflow has been experimentally investigated [10,9]. The experimental setup (Fig. 2 (left)) was composed of a horizontal channel with a square section of 160×160 mm, two tanks filled with particle suspensions for the LIF/PIV measurements and two pumps producing the jet and the crossflow. The square jet of 30 mm width flows from bottom to top. In the channel, the mean flow velocity is fixed to 1.7 cm/s in order to have the Reynolds number $Re = 500$. The measurement techniques are represented in Fig. 2 (right). The velocity and concentration fields are respectively measured by a PIV (Particles Image Velocimetry) 3D technique and a LIF (Laser Induced Fluorescence) 3D technique. The PIV3D technique uses 0.001-mm diameter silver-coated hollow glass spheres. The LIF3D technique uses Rhodamine 6G (10^{-7} mol/L). The velocity and concentration fields are estimated by analyzing the pictures which are taken by means of two Lavision high-speed cameras.

4. Results

4.1. Non-zero divergence

The measured 3D experimental velocity field has been used in the numerical simulations. The problem of the non-zero divergence (i.e. $\nabla \mathbf{u} \neq 0$) is clearly identified in Fig. 3, where the approximated 3D concentration field of inert tracer particles $c_h(\mathbf{x}, t)$ obtained by means of the particle method is plotted in the median plan. Corresponding to a coarse repartition of numerical particles, zones of higher and lower concentrations appear. Fig. 4 presents in the median plan the divergence $\mathrm{div}(\mathbf{u}(\mathbf{x}, t))$, computed from the measured 3D experimental velocity field. Zones of positive and negative divergences are observed. As it could have been expected, the experimental setup does not provide flow fields with a zero divergence because of the experimental errors. The deviations of computed particle trajectories give a direct representation of the non-zero divergence. Actually, the experimental errors on the fields of concentration and velocity do not have any straightforward correlation. Moreover, the concentration field is a direct result of the LIF, whereas the PIV measurement requires a numerical treatment. Therefore, it is expected that the numerical error can be pointed out by comparisons of the computed and measured concentrations.

4.2. Efficiency analysis

The initial condition of the 3D numerical concentration field of inert tracer particles c_h $(\mathbf{x}, t = 0)$ has been imposed with the 3D experimental concentration field measured at time $t = 0$ s. The initial number of numerical particles $\mathcal{N}_p$ and the regridding frequency $\mathcal{N}_f$ are respectively equal to 316,835 and 1 [11]. For all the numerical results, a time step $\delta t = 0.001$ s was selected. Figs. 5 and 6 present the 3D concentration field and its projection in the median plane together with the isosurface 0.2 mg/l obtained from the experimental data at time $t = 7.5$ s. The particle method and the two variants of the

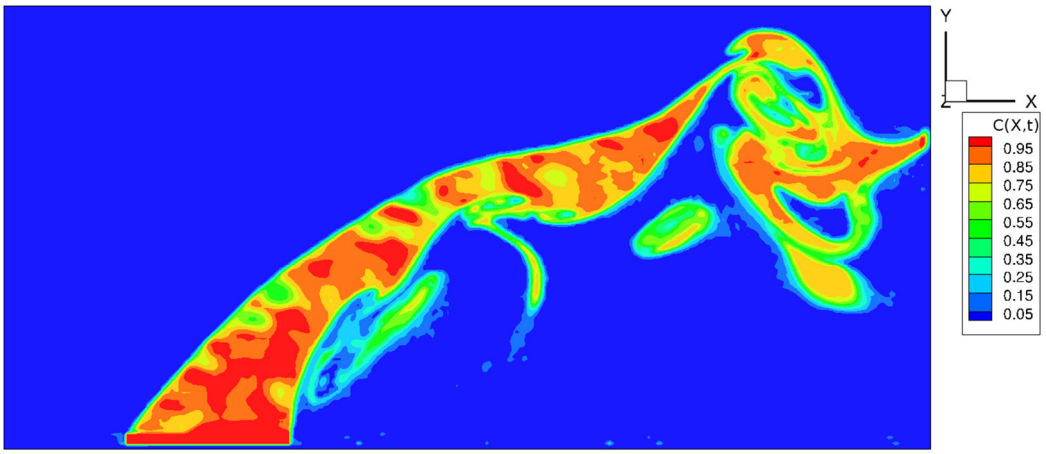

Fig. 3. 3D numerical concentration field of inert tracer particles $c_h(\mathbf{x}, t)$ represented in the median plan and obtained by means of the particle method by using the 3D experimental velocity field at time $t = 0.06$ s.

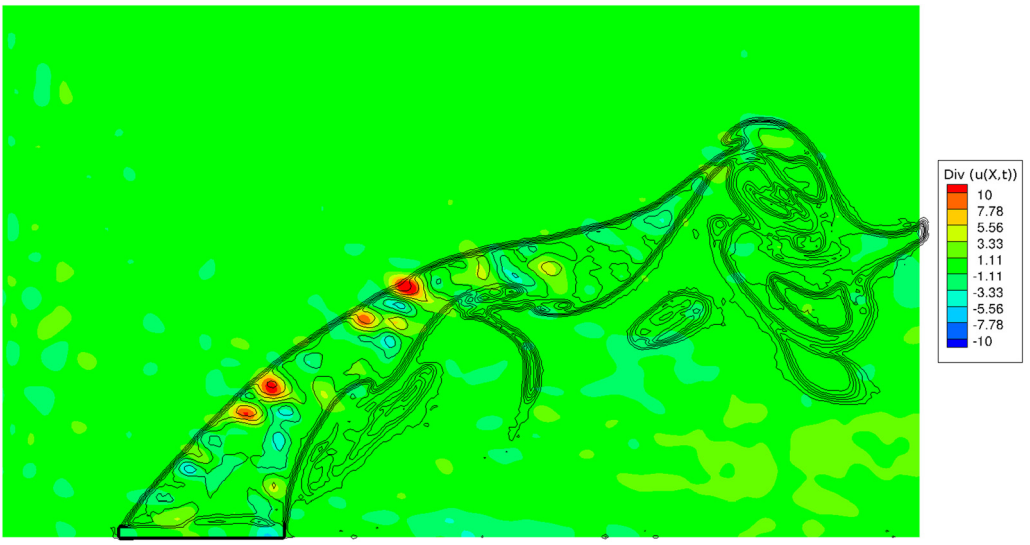

Fig. 4. Overlapping of the 3D experimental divergence field div($\mathbf{u}(\mathbf{x}, t)$) (color map) and the 3D numerical concentration field of inert tracer particles $c_h(\mathbf{x}, t)$ (contour lines) at time $t = 0.06$ s.

corrected particle method were used: the DMF (Divergence Mass Flux) and the RSF (Renormalized Smoothing Function). The efficiency of both correction methods can be pointed out. The particle method fails to reproduce the measured results, whereas DMF and RSF yield almost the same results and they are very close to the experimental data. The zones of higher and lower concentrations are no longer apparent for both corrections, DMF and RSF. In order to further investigate the methods, an error estimate $\mathcal{E}r_2$ was computed:

$$\mathcal{E}r_2(t) = \frac{\sum_i^M (c_h(\mathbf{x}_i, t) - c_e(\mathbf{x}_i, t))}{\sum_i^M (c_e(\mathbf{x}_i, t))} \tag{12}$$

where M is the number of numerical particles with $C_i \geq 10^{-6}$, $c_e(\mathbf{x}_i, t)$ the experimental concentration field and $c_h(\mathbf{x}_i, t)$ the numerical concentration field. In Fig. 7, the logarithm of the error $\mathcal{E}r_2$ has been plotted as a function of time t for the two corrections, DMF and RSF. The error $\mathcal{E}r_2$ grows constantly up to 4 s, where it seems to reach a plateau. The error $\mathcal{E}r_2$ is then about 0.75. The two corrections have the same behavior. The influence of the time step δt was also investigated. Two time step values were used, $\delta t = 0.001$ and 0.01 s. Fig. 8 presents the 3D numerical concentration field $c_h(\mathbf{x}, t)$ in the median plane at time $t = 7.5$ s obtained with the correction DMF for these two values. We can observe that the best results were obtained with the smaller time step for the correction DMF. On the other hand, the results were almost unchanged for the correction RSF.

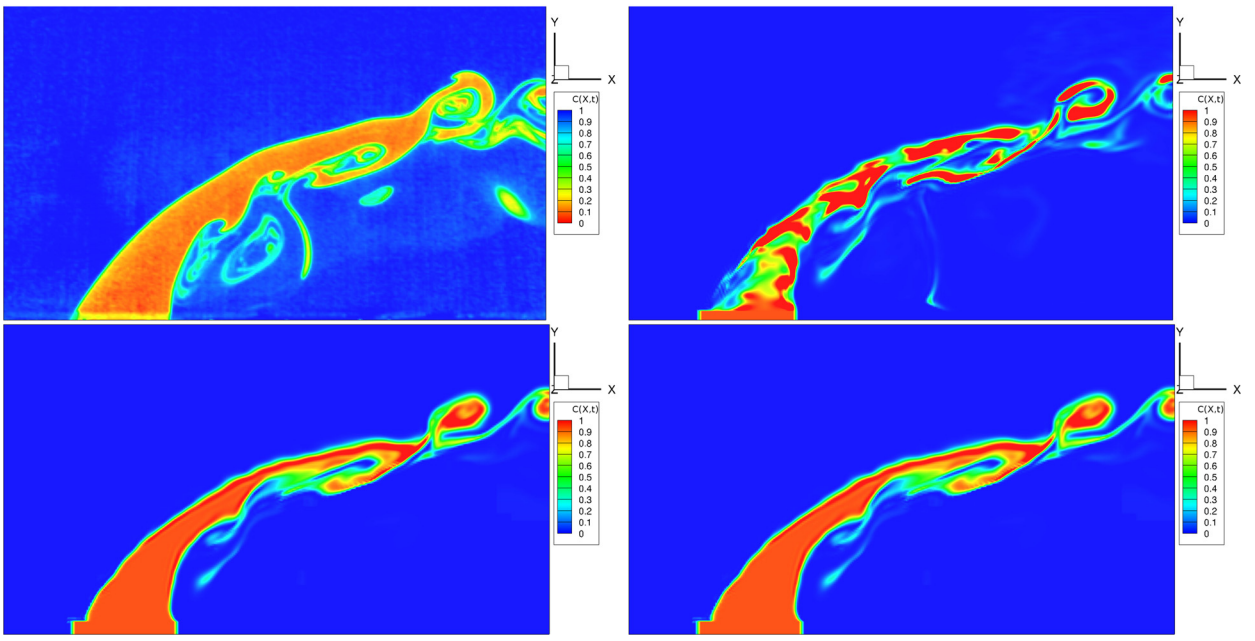

Fig. 5. 3D concentration field of inert tracer particles, represented in the median plan at time $t = 7.5$ s, obtained from the experimental data (left top), the particle method (right top), the DMF correction (left bottom) and the RSF correction (right bottom).

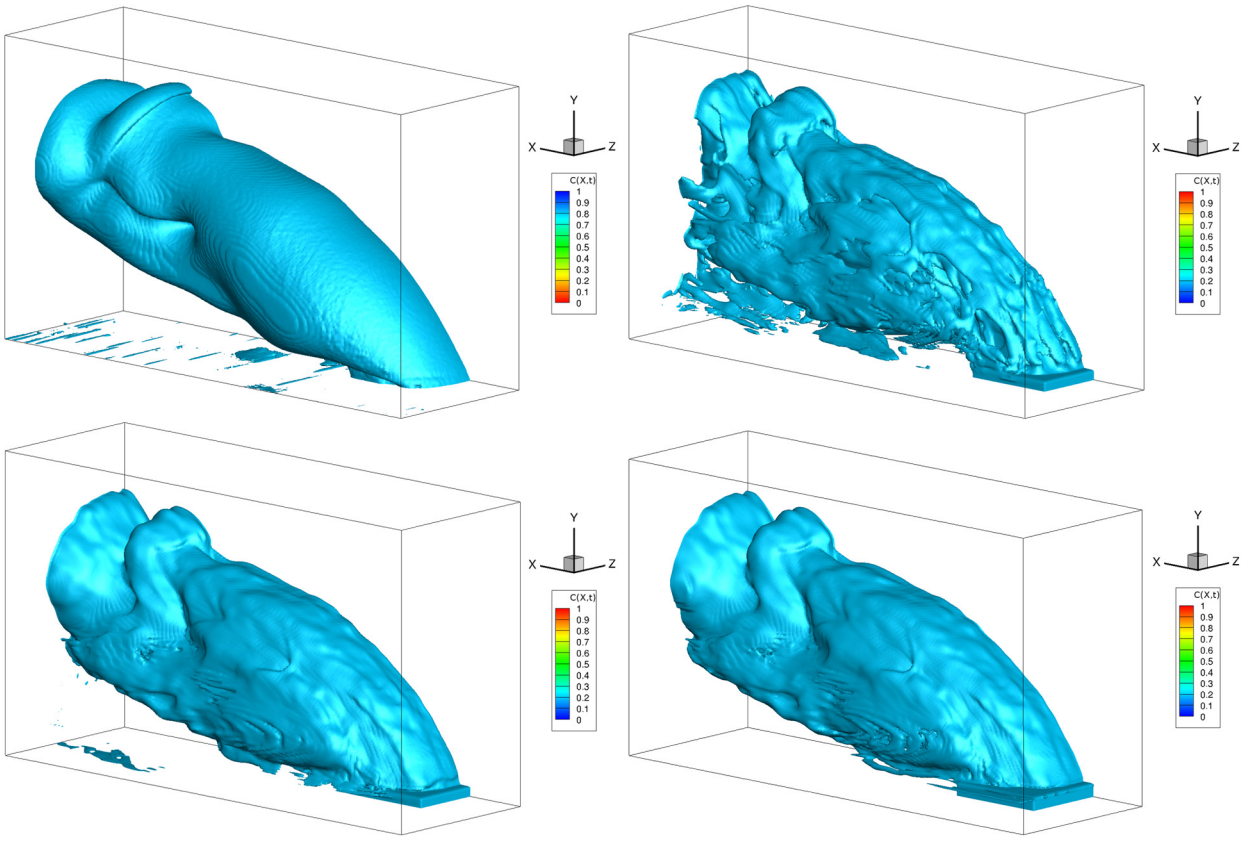

Fig. 6. 3D concentration field of inert tracer particles, represented by the isosurface 0.2 mg/l at time $t = 7.5$ s, obtained from the experimental data (left top), the particle method (right top), the DMF correction (left bottom) and the RSF correction (right bottom).

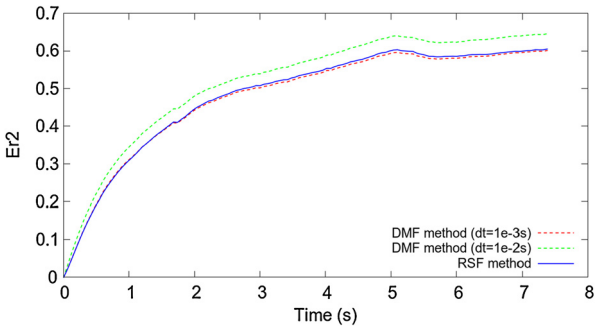

Fig. 7. Error $\mathcal{E}r_2$ with respect to time t, obtained with the DMF correction (dashed line) and the RSF correction (solid line).

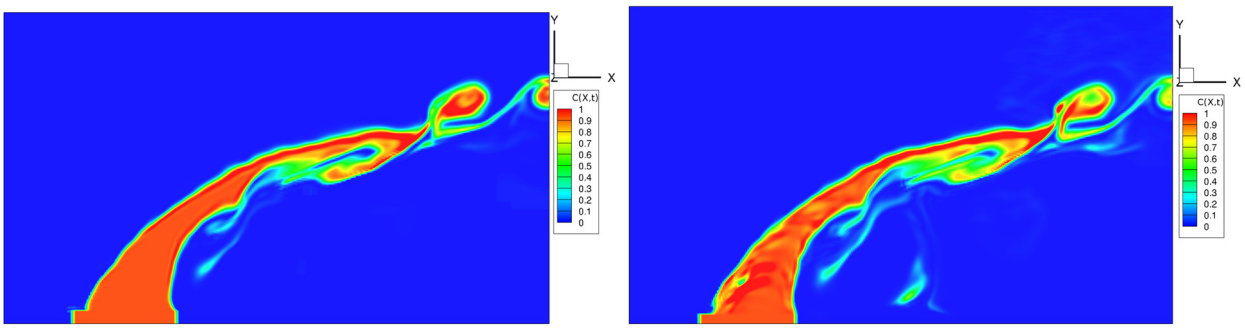

Fig. 8. 3D numerical concentration field of inert tracer particles $c_h(\mathbf{x}, t)$, represented in the median plan at time $t = 7.5$ seconds, obtained for two values of the time step, $\delta t = 0.001$ s (left) and 0.01 s (right) with the DMF correction.

5. Conclusion

In this paper, the relation between the non-zero divergence of flow fields and the approximated concentration error was established. Two corrections of the particle method, DMF (Divergence Mass Flux) and RSF (Renormalization Smoothing Function), were designed to correct this effect. The DMF correction results in a modification of the particle weight through a differential equation. As a result, it was found to be sensitive to the time step. The RSF correction was found to provide better results although it could be questionable whether this property can be conserved for long time calculations or not, because of the distortion of the grid distribution.

References

[1] T. Kitada, Effect of non-zero divergence wind fields on atmospheric transport calculations, Atmos. Environ. 21 (4) (1987) 785–788.
[2] M.A. Nunez, R. Mendoza, Structural instability of atmospheric flows under perturbations of the mass balance and effect in transport calculations, in: VIIth International Congress of Engineering Physics, J. Phys. Conf. Ser. 582 (2015).
[3] C.R. Anderson, C. Greengard, Vortex Dynamics and Vortex Methods, American Mathematical Society, 1991.
[4] G.H. Cottet, P.D. Koumoutsakos, Vortex Methods: Theory and Practice, Cambridge University Press, 2000.
[5] R.A. Gingold, J.J. Monaghan, Smoothed particle hydrodynamics—theory and application to non-spherical stars, Mon. Not. R. Astron. Soc. 181 (1977) 375–389.
[6] Z. Chena, Z. Zongb, M.B. Liud, L. Zoub, H.T. Lib, C. Shua, An SPH model for multiphase flows with complex interfaces and large density differences, J. Comput. Phys. 283 (2015) 169–188.
[7] J.T. Beale, On the accuracy of vortex methods at large times, in: Computational Fluid Dynamics and Reacting Gas Flows, in: The IMA Volumes in Mathematics and Its Applications, vol. 12, 1988, pp. 19–32.
[8] P. Ploumhans, G.S. Winckelmans, J.K. Salmon, A. Leonard, M.S. Warren, Vortex methods for direct numerical simulation of three dimensional bluff body flows: application to the sphere at $Re = 300$, 500 and 1000, J. Comput. Phys. 178 (2002) 427–463.
[9] A. Berchet, L. Thomas, P. Braud, L. David, Instantaneous volumic concentration and velocity measurements of a jet in crossflow for the evaluation of the entrainment, Exp. Fluids 54 (12) (2013) 1608.
[10] R. Vernet, L. Thomas, L. David, Analysis and reconstruction of a pulsed jet in crossflow by multi-plane snapshot POD, Exp. Fluids 47 (2009) 707–720.
[11] A. Jolles, S. Huberson, Correction of the projection error in particle mesh methods, Rech. Aérosp. 4 (1990) 1–6.